International Journal of Innovative Technology and Exploring Engineering (IJITEE)
ISSN: 2278-3075 (Online), Volume-9 Issue-2, December 2019

Photocatalytic Performances and Antibacterial Activities of Nano-Zno Derived By Cetrimide-Based Co-Precipitation Method by Varying Solvents

S. Sheik Mydeen , M. Kottaisamy V.S Vasantha

Abstract: ***In this work, zinc oxide nanoparticles have been synthesized by cost-effective and based on the efficient cetrimide and varying solvents are using the method of co-precipitation annealing at 350 °C. The resultant powder samples were characterized well by means of XRD, SEM, FT-IR, PL and UV-visible DRS spectroscopy. Among them, XRD exhibits ZnO has the structure of hexagonal wurtzite with a preferred orientation of 101 planes. It is noted in ZnO represented in SEM images have different solvents and cetrimide has a strong influence on the morphology of ZnO nanostructures that are to be sized are 50nm, 70nm, 90nm 100nm. It confirms that the changes in the band-gap from UV-vis DRS data. The presence of Zn-O confirms various functional groups decomposed in the sample from FTIR data. The PL study states that the emission band available at approximately 410nm and checks the recombination level shows low, further, it correlates with good photocatalytic properties. The sunlight measured by Lux meter and dye degradation studies is done by a simple aeration photocatalytic technique represents 95% degradations and under UV light is 85%. Besides, the scavengers of the responsive species of during the degradation were additionally examined for photocatalytic mechanism. An antibacterial activity is enhanced significantly, which is based on the attribution of Nano features of ZnO nanostructures for p. aeruginosa bacteria. Thus, this study paved the way for potential applications of photocatalytic and antibacterial activities.***

Keyword: ***Among them, XRD exhibits ZnO has the structure of hexagonal wurtzite with a preferred orientation of 101 planes.***

I. INTRODUCTION

Environmental pollution is one of the major hazards to human, animal life and environment [1]. The industrial effluents contain organic dyes which are highly toxic, non-biodegradable and carcinogenic materials [2].

Revised Manuscript Received on December 30, 2019.
***** Correspondence Author
S. Sheik Mydeen, Department of Chemistry, Sethu Institute of Technology, Pulloor, Kariapatti, Tamilnadu, India.
M. Kottaisamy Department of Chemistry, Thiagarajar College Engineering, Madurai, Tamilnadu, India.
V.S Vasantha*, School of Chemistry, Madurai Kamaraj University, Palkalai Nagar, Madurai, Tamilnadu, India

Generally, organic dyes are applied in the industries like paper, textile, solar cell, medicinal and plastic industries. Such industrial effluents are, before, being discharged into the environment, the pollutants need to be removed and make them into acceptable quality [3]. The waste water contains organic pollutants can be degraded by Photocatalytic degradation method and it has a good efficiency, comfortable operation, inexpensive process and preferably making nontoxic final products [4-6]. The photo-degradation procedure uses efficiently accessible semiconductors which prompt, complete degradation of natural products to CO_2, water, and mineral acids [7]. The ZnO nanomaterial is more economical for the treatment of organic dye than other semiconductor materials [8-11]. Since the space group of ZnO its P63mc, and a lattice parameter value of a = 0.3245 nm and c = 0.5209 nm is a significant II-VI and n-type semiconductor that has a wide-ranging band gap value of 3.37eV the formation of nano-ZnO involves a hexagonal wurtzite structure 12. In the past decades, ZnO nanoparticles synthesized by using different techniques such as sol-gel, ball milling, hydrothermal process, combustion technique and co-precipitation methods. The ZnO nanoparticles prepared by the various methods differ in their properties, which is mainly due to synthesis procedures [13]. The co-precipitation the technique is an alternative procedure for the preparation of ZnO nanoparticles at room temperature for photo catalytic properties because of its simple, economical and easy process [14]. However, quality of prepared nanoparticles highly depends the nature of the precursor solution of higher order homogeneity and chemical stability. In order to change the morphology, size and shape for avoiding agglomeration of nanoparticle use surfactant is the best way for preparation of nanoparticles. One of the efficient surfactants for the preparation of nanoparticles of ZnO using Cationic surfactant [15].The current work adopted very fast and facile strategies to improve the morphology of nano-ZnO. Some surfactants or organic solvents used to control the size of nanoparticles and its consequences on dye degradation characteristics [16]. The impact of surfactant with different solvent and the changes in morphology of ZnO nanoparticles was investigated with the help of XRD, SEM, FTIR, PL and UV–visible spectroscopy investigation techniques. In particular, the influence of the surfactant and solvent on the photocatalytic behavior of nano-ZnO also the possible mechanism of Methylene blue (MB) dye-degradation is also proposed.

In the dye industry, the pH of effluent is about 9. So, the dye degradation was carried out at pH 9.

The antibacterial assays were performed on different microorganisms like Pseudomonas aeruginosa, staphylococcus aureus, salmonella typhi and bacillus subtilis by the standard agar disc diffusion method.

II. EXPERIMENTAL

Materials Required

Zinc acetate dehydrate was purchased from Merck 99% (Zn $(CH3COO)_2$•$2H_2O$) and 99% Cetrimide (surfactant), ethanol 99.9%, sodium hydroxide 98%, and methylene blue (MB) 98%. All the chemicals are purchased at analytical grade and utilized as received. The double distilled water is used for the preparation of ZnO and dye solutions.

ZnO nanoparticles preparation

0.15 M of Zinc Acetate dihydrate and 0.05 M of Cetrimide ($C_{17}H_{38}BrN$) were dissolved in an appropriate amount of water. This solution was stirred at room temperature for 2 hours, 1.2 M of sodium hydroxide solution was added into the above solution in drop wise. After centrifugation, the resultant precipitate is washed with double distilled water and liquid ethanol, then the resultant precipitate was dried at the 60^{o}C. The dried precipitate was transferred in the agate mortar and then ground well. Lastly, it has annealed at 350°C in a muffle furnace for 2 hours and then allowed for slow cooling to reach at the room temperature. The flow chart shows the detailed synthesis process of nanoparticles (named as SA1), the same procedure was followed in the remaining samples, namely SA2, SA3 and SA4 for different combination of solvents such as water with Cetrimide, ethanol and ethanol with Cetrimide respectively as shown in Figure 1.

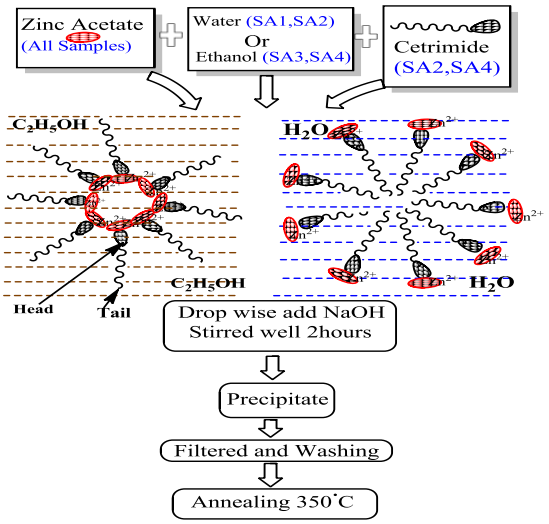

Figure 1. Synthesis of ZnO nanoparticles (SA1, SA2, SA3 and SA4)

Characterization

Powder X-ray diffraction was carried out using PAN analytical of X-ray Diffractometer using Cu Kα source (λ=1.5418 Å) to confirm the crystalline nature of ZnO samples. The FTIR spectrum of ZnO samples was recorded by SHIMADZU 8400 FTIR Spectrometric Analyzer instrument using KBr pellet methods and the range of 400-4000 cm^{-1}. The Photoluminescence (PL) study has recorded at room temperature utilizing Varian Cary Eclipse Spectrophotometer. The surface morphologies of ZnO samples have been studied by scanning electron microscope (SEM VEGA3 TESCAN). The elemental analysis is done by EDX spectrometry instrument (Brucker Quantax 200 AS). To analyze band gap, Shimadzu UV-2450 Spectrophotometer type of UV diffuse reflectance spectra (DRS) was utilized.

Photocatalytic Analysis

The photocatalytic properties of ZnO were calculated by monitoring the speed of degradation of MB in a UV lamp (30 W, 365 nm, Philips TL-D K 30W, ACTINIC BL, Hg) a home-made apparatus and solar radiation source. In this, each photocatalytic experiment was carried out by 100 ml reaction bottle, 0.25 gm of ZnO photocatalyst was spread in 100 ml of 100 ppm of MB solution and prepared using distilled water. The solution containing ZnO suspension was agitated by fish motor aeration in the dark for 30 mins. Then the MB solution was exposed to the sunlight and UV-lamp light source radiation, then 5 ml of the sample utilized in the uniform time interval of 1 hour. The sample solution was centrifuged and filtered, finally, then the supernatant solution was collected and diluted to 10 times, then further analyzed different concentrations of MB using UV-Vis spectrophotometer. The characteristic absorption peak of MB observed at 663nm was monitored.

Antibacterial assays

The antibacterial evaluations were performed on different micro-organisms such as gram-positive bacteria's(G.P) (staphylococcus aureus and bacillus subtilis) and gram-negative bacteria's(G.N) (Pseudomonas aeruginosa and salmonella typhi) by using disc diffusion method. The cultivation of bacterias was done by the medium of Luria Bertani (LB) broth/agar. Luria agar plates spread of the culture of inoculums (50 µl) during overnight. In diffusion method, discs of 5 mm diameter used to keep 30 µg/ml samples along with standard antibiotic (30 µg/ml) were positioned in every plate as a control. All Plates were incubated at 37 °C for overnight. The inhibition zones were measured on the next day around the discs.

III. RESULTS AND DISCUSSION

X-Ray Diffraction Analysis

The Figure 2 shows the XRD pattern of all the preparations of ZnO samples. All the obtained diffraction peaks were in good promise with a characteristic wurtzite type ZnO nano crystal structure (hexagonal, JCPDS No. 36-1451). There were no other diffraction peaks for impurities in the XRD patterns of all the samples. The spectra of pure ZnO nanoparticles show the sharp several peaks (100), (002), (101), (102), and (110) planes. Singh et al. discuss the edge of the sharp peaks reveals a great level of crystallinity of the prepared ZnO nanoparticles [17].

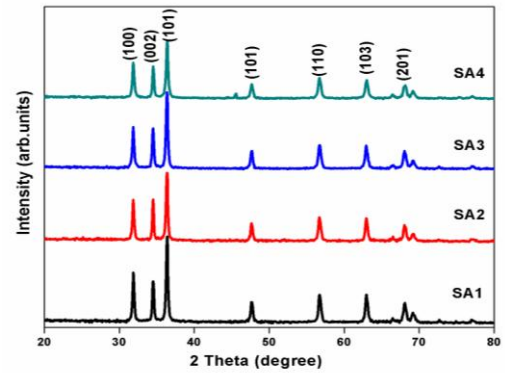

Figure 2- XRD pattern of all the preparations of ZnO samples

Figure 2. shows the XRD graph of ZnO nanoparticles prepared using solvents and surfactants such as Water (SA1), water with a Cetrimide (SA2), ethanol (SA3), and ethanol with Cetrimide (SA4).

XRD peak intensity and half width reveal that all the synthesized samples have a well-defined crystalline structure at room temperature. The marginal changes in intensity of different peaks indicate the influence of solvents viz., Water, ethanol and cetrimide.

The average crystallite size (D) of nano-ZnO was calculated using Debye-Scherrer equation [18],[19].

$$D = \frac{0.9\lambda}{\beta\cos\theta}$$

Here, the wavelength is λ and the X-ray Cu Kα radiation 1.54056 A°, β is a half the maximum intensity [half width full maximum], and the Bragg's diffraction angle in radians is θ.

A micro strain (ε) of nano-ZnO is calculated from this expression [20],[21].

$$\varepsilon = \frac{\beta\cos\theta}{4}$$

The dislocation density (δ) value was calculated and using the procedure in relation 20.

$$\delta = \frac{1}{D^2}$$

The sample SA2 shows the smaller crystallite size (higher defects) as shown in Table 1, SA4 is, thus, representing the improvement of crystallinity of the nanoparticles. The crystallinity improvement led probably to decrease the strain of ZnO nanoparticles [22].

Table 1. XRD data to find Crystal size, Micro strain and Dislocation density

Sample	Crystal Size D nm	Micro strain ε x 10-4	Dislocation Density δ x 10 14 (lines/m^2)
SA1	33.00883	14.26298	0.92
SA2	31.09346	15.37	1.0
SA3	31.47229	14.98	1.0
SA4	36.18741	13.48626	0.76

FTIR spectroscopy

Configuration molecular species change and decomposition compound were studied using Fourier Transformed Infrared Spectroscopy. As shown in Figure 3 the synthesized ZnO nanoparticles analysis by 400-4000 cm^{-1} range of FTIR spectrum. In the region 2800-3000 cm^{-1} no bands are observed and attributed to absence of Cetrimide surfactants [23], [24]. The results indicate that Cetrimide has been decomposed at higher temperatures in all nanoparticles. The acetate group band appearing in 2381cm^{-1} are clearly recognized during the vibration mode of CO_2 stretching of asymmetric and symmetric. The peak 1400-1500 cm^{-1} region has sharp bands recognized to the molecular deformation and the formation of the vibrations of C=C, C=O at the assimilated Cetrimide surfactants in nanoparticles of SA2 and SA4. The peak at 847 cm^{-1} is C-H stretches indicate the long chain cetrimide. The IR band of Zn-O bonding corresponding to the ZnO nanoparticle is observed at 438 cm^{-1} ***[25]*** . There is a broad band near at 3400cm^{-1} correspond to stretching, vibration modes of OH group, indicating some water molecule adsorbed on ZnO crystal surfaces at the nanoparticles is SA2, SA3, SA4. These three nano samples attribute to the force of attraction between water- cetrimide, ethanol - water, Ethanol, cetrimide and water, respectively. The SA4 sample has surfactant strongly bound with ZnO with presence of ethanol by representing peak of 1500cm^{-1}.

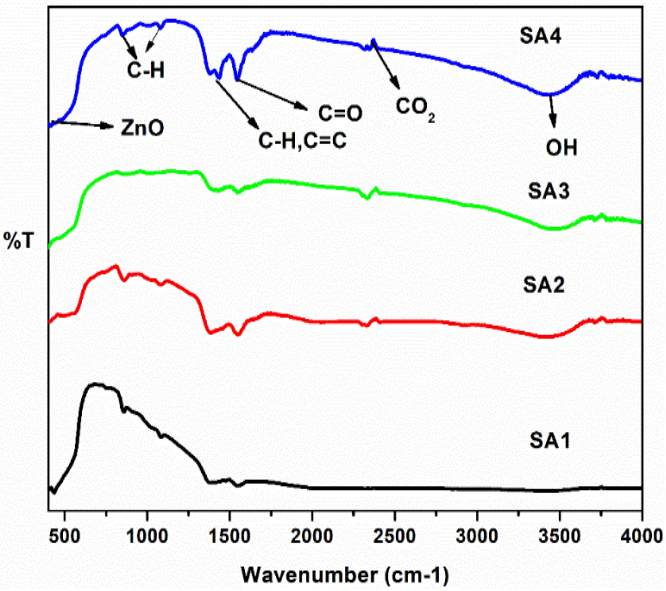

Figure 3. FTIR analysis of ZnO nanoparticles prepared with different solvents Water (SA1), water with a Cetrimide (SA2), ethanol (SA3), and ethanol with Cetrimide (SA4).

DRS spectroscopy

The photocatalytic study of nano-ZnO analyzed from UV-Vis diffused reflectance data seen in Figure 4. The UV-Vis DRS spectra of nano-ZnO (SA1 and SA3) was found at 375nm, while the other samples of nano-ZnO (SA2 and SA4) had shown the reflectance spectra at 365nm and 370nm, respectively with blue shift which may be due to the presence of surfactant during synthesis. The band gap energy of nano-ZnO is calculated using the formula follows.

$$Eg(eV) = hc / \lambda = 1240 / \lambda$$

Where, Eg is the band gap energy (eV), h is Planck's constant, c is the velocity of light and the wavelength is λ (nm) of absorption onset [26]. The band gaps SA1, SA2, SA3 and SA4 are 3.31eV, 3.4eV, 3.31eV and 3.35eV, respectively. In the case of SA2 and SA4, the band gap of zinc oxide value is different due to the presence of surfactant during synthesis.

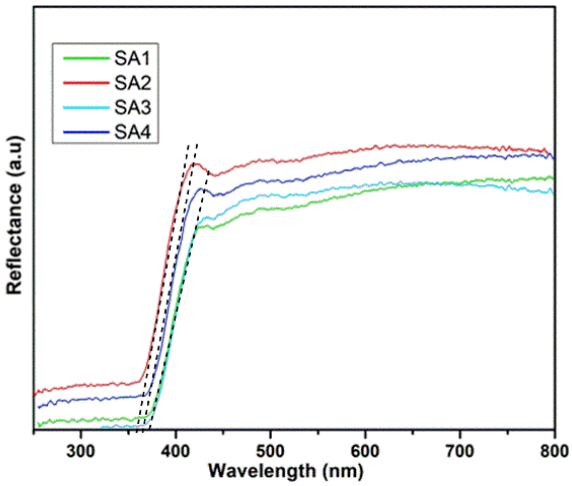

Figure 4. UV visible DRS studies of ZnO Nanoparticles prepared with different solvents (SA1) Water, (SA2) Water with Cetrimide, (SA3) Ethanol and (SA4) Ethanol with Cetrimide.

Photoluminescence Spectra

Photoluminescence spectra is a fundamental instrument to examine the electron/hole pair recombination procedure happening in a semiconductor. The excitation wavelength of 375 nm and the resultant spectra are appearing in Figure 5. The emission peak at 410 nm, the ZnO samples have absorbed the photons with sufficient energy to create the electron/hole and the energy released when the recombination of charge carrier. Ku et al. said this is essentially different redox energy levels of the valence and conduction band of the ZnO, which lead to the reduces the electron and hole recombination by interfacial electron charge transfer [27].

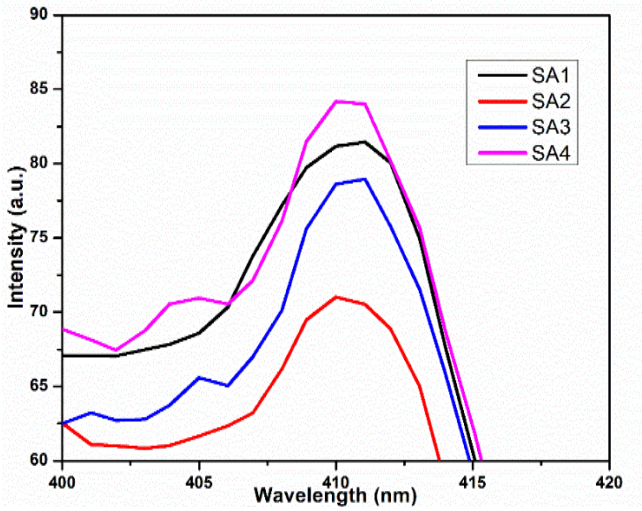

Figure 5. Photoluminescence spectra of SA1, SA2, SA3 and SA4 and the excitation wavelength was 365 nm.

Surface Morphological Studies

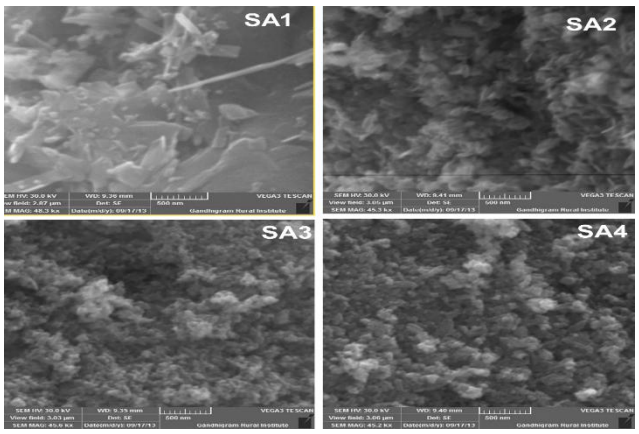

Figure 6.SEM images of ZnO nanoparticles prepared using (SA1, SA3) Water and ethanol assisted SEM images of the Zinc Oxide, (SA2, SA4) Water and Cetrimide, Ethanol and Cetrimide assisted.

The progress of crystal morphology is affected by Solvent and are well-recognized in organic chemistry. Weissbuch et al, reported the solvent-surface interactions are generally understood in various types such as Vander Waals force, hydrogen bonding, electrostatic attraction [28]. Some solute molecules are hampered at specific crystal face interactions with inhibit the agglomeration and on the growth of crystal faces. The different surface morphology of ZnO nanoparticles is prepared in four-way method such as ethanol and water with and without surfactant i.e. cetrimide Figure 6.

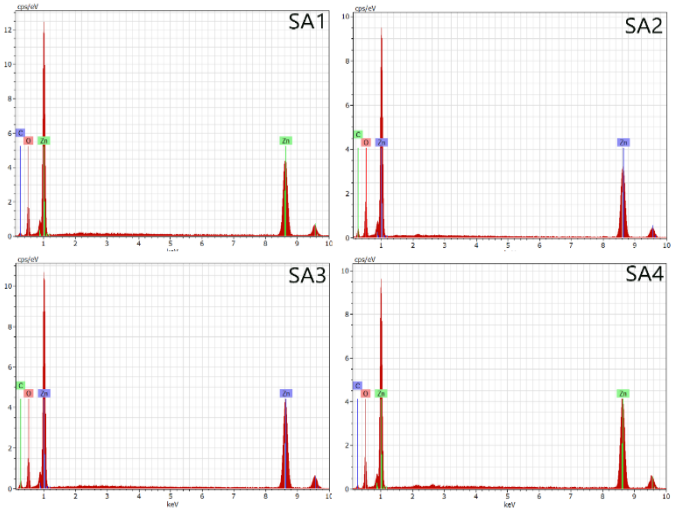

Figure 7. EDX pattern of ZnO nanoparticles (SA1, SA2, SA3 and SA4)

Prepared SA1 using water indicates agglomeration to pin like structure and particle size in the range of 250 nm length and 100 nm breadth. The sampled SA2 prepared in water and surfactant indicates the thread like structure and particle size is 180 nm length and 50 nm breadth. The sample Cetrimide prepared in ethanol SA3 sample depicts sponge like structure, then, the particle size is 120 nm length and 70 nm breadth. Finally, SA4 sample is synthesized in ethanol and the surfactant Cetrimide is rice like structure and the particle size is 250 nm length and 90nm breadth.

The synthesized SA2, SA3 and SA4 nanoparticles are homogeneous structure and distributed uniformly throughout the sample. The ZnO growth process is different for solvent in the presence of cetrimide shows Figure 1. The cetrimide is a long chain cationic compound, which ionizes completely dissolved in water also. This cation part is the hydrophilic head positively charged tetrahedron with a long hydrophobic tail in the water solvent but cetrimide behaves in ethanol solvent, long hydrophilic tail with a hydrophobic head. So that SA2, SA4 particle size and shapes are varied depends on the solvent and Surfactant interaction [29]. The surface tension of water is nearly triple times higher than ethanol solution and solvent interaction are variable. Water and Ethanol is a very polar molecule, but ethanol, organic molecule has a polar response of hydroxyl (OH) group and other end of a non-polar alkyl group of ethyl (C_2H_5) in ethanol, consequently, information is changing particle size and shape of sample SA1 and SA3.

Table 2. EDAX data for nano ZnO

Atom%	SA1		SA2	SA3	SA4
Oxygen	50.85		46.89	42.57	50.29
Zinc	49.15		53.11	57.43	49.71

EDAX analysis is helping to analyze the any elemental composition of ZnO all nanoparticles. Figure 7 shows the electron density distribution of different orbital states of zinc and oxygen of the as prepared Nanoparticles. This graph reveals about the prepared ZnO samples has no other elements, primary O. Table 2 shows the SA2and SA3 samples in Zn and Oxygen composition compare, the Zn percentage is higher than the oxygen for SA2 and SA3 samples. The result reveals that the oxygen vacancy is present in the surface of the nanoparticles, furthermore, the carbon peak indicates the sample preparation of SEM analysis.

IV. PHOTO CATALYTIC REACTOR AND STUDIES

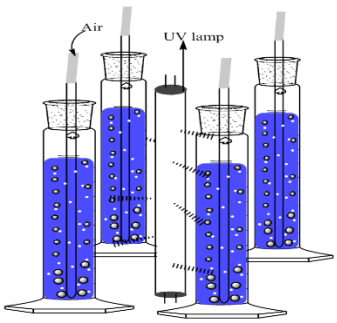

Figure 8. Schematic representation on study of degradation of methylene blue under UV light.

For an estimation of the photo-catalytic action of the ZnO nanoparticles and degradation of methylene blue solution was undertaken. The UV light degradation setup process is, the UV light is centered and Surrounded by all Photocatalytic reactors (100ml reaction bottle) kept in standing 4cm distance between UV light and simultaneously degrade all samples of SA1, SA2, SA3 and SA4. Using fish tank motor, the air supply tube is connected to a glass tube in the reactor that helps air to keep agitated with Nano ZnO and help to involve photocatalytic mechanisms associated to ZnO and demonstrated in UV light setup Figure 8. The Sun light degradation setup same as UV light and photo reactors focused standing in Sun light direction Figure 9.

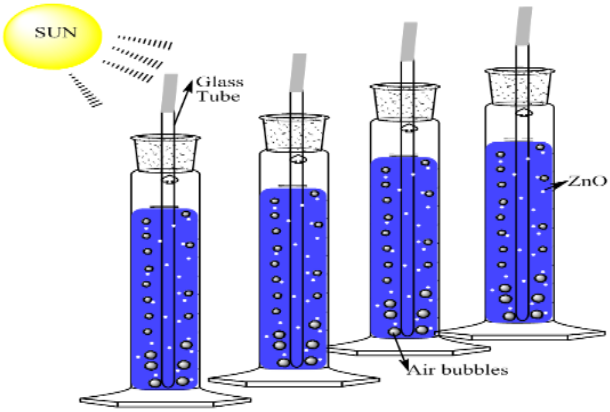

Figure 9. Schematic representation on study of degradation of methylene blue under sunlight.

An experiment consists of 3cm diameter of glass reactor contains 100 ml of 100 ppm dye solution, then add NaOH to raise up to pH 9 and 0.25 g of catalyst. This MB solution was treated by UV light of 30 W and UV bulb, with the wavelength of 365 nm. The atmospheric oxygen passed through via a glass tube in a reactor container by using fish tank motors. The air is pumped at the speed of 1litre/40 seconds. The passing air helps us keeping the catalysts in suspension and also involving in the photo degradation mechanism reaction. The light source and reactor distance are 4cm. Another degradation source of solar light irradiation in this experiment was carried out the summer duration between 9 am to 5 pm with noted solar flux intensity Figure 10c.

The MB and catalyst mixture were stirred in the dark room for 30 minutes when dye molecules develop the adsorption equilibrium between catalyst surfaces. Then, the light is illuminated on the reactor, decolorization of dye molecules occurred, moreover, the rate of decolorization increased due to availability of active sites like peak, corner, defects etc. So, catalyst surface increases adsorbed number of dye molecules [30]. The photo-catalyst activity sample SA1 and SA4 MB degradation are slow compared to SA2 and SA3samples. The reason is high catalytic activities of the sample SA2 and SA3 may be due to their thread and sponge like structures, respectively Figure 10a. The SA2 and SA3 samples exposed to the sunlight due time it degrades the methylene blue solution, finally, the complete discoloration process was achieved within 360 minutes and reach MB degradation is 95%. The morning sunlight Lux values were low, even though well adsorption is found initially and degradation occur in MB as a result the degradation is fast. Then, afternoon 12 pm to 2 pm higher degradation is found due to the high flux intensity of sunlight in Figure 10b,c.

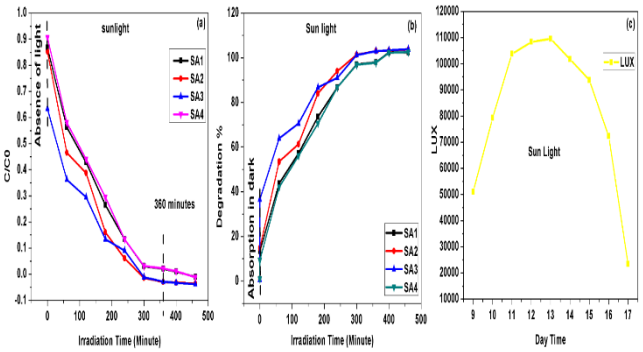

Figure 10. (a) and (b) The ZnO catalytic activity of degradation of MB under sunlight irradiation, (b) Day time Lux intensity of sunlight at the time of Photo

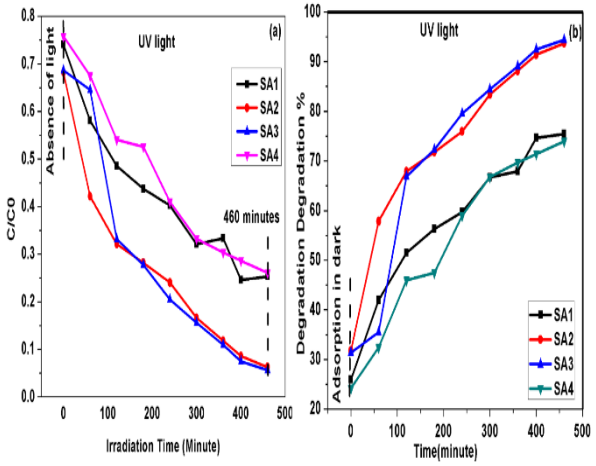

degradation.

Figure 11. (a) and (b) The ZnO catalytic activity of degradation of MB presence of UV light irradiation

In UV initial light irradiation time, all ZnO samples have higher degrade than the MB, later, gradually slow down the degradation still 460 minutes of 85% of MB degrade Figure 11a, b. When comparing UV and sunlight, the UV light has the same intensity from starting to the end of the reaction, but the Sunlight Lux intensity value varies, it means increasing then decreasing accordingly.

Photocatalyst Mechanism

Li et al. reported that photocatalytic response incorporates photoexcitation of electron by and large, charge division and relocation, and surface oxidation– reduction reactions [31]. The UV light is illuminated when the reactive species produced the photocatalysts are h^+, $^{\bullet}O_2^-$ and $^{\bullet}OH$. It has comprehended the ZnO mechanism for degradation of MB dyes, it is important to recognize which receptive species assumes a noteworthy job in the photocatalytic degradation method. The observation is the absence of holes, the degradation rate is reduced. So that hole (h^+) is mainly involved in photocatalytic degradation MB dye than $^{\bullet}O_2^-$ and $^{\bullet}OH$. This result correlates the PL spectra describe the h^+ hole recombination inhibition of electron. The $^{\bullet}O_2^-$ scavengers result connected with EDX spectra attribute the surface oxygen vacancy of nanoparticles.

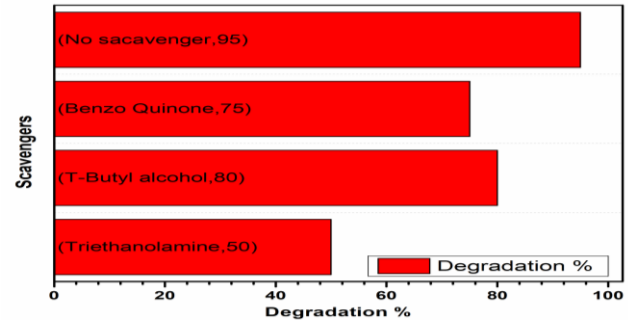

Figure 12. Removal of MB over ZnO in the presence of various scavengers (75 min irradiation time, 0.25gm/L of ZnO, initial concentration MB is $2x10^{-5}$ M and pH = 6.8)

In light of the above outcomes, the fundamental mechanism of photocatalytic degradation of MB pollutants over ZnO under light illumination is proposed in Scheme Figure 13. These shifted electrons are adsorbed (scavenger) by an oxygen molecule to give the superoxide radical $^{\bullet}O_2$. This •OH radical is an enormously good oxidant for the degradation of MB [35, 36]. The Photo catalytic studies carried out for the prepared samples at all together.

Table 3. Comparison of degradation of MB using different nano particles

Light source	Catalyst	Concentration (MB)	Duration	% degradation	Reference
Sun Light	0.010g ZnO	5 ppm	165 min	100	[37]
Sun Light	0.025g ZnO	10 ppm (pH 6.3)	90 min	100	[38]
Visible light	0.01g ZnO (H202)	1X10-5 M (pH7)	210 min	100	[39]
UV-Visible	1.5 g ZnO	10 ppm (pH7.7)	25 min	98	[40]
UV-Visible	0.25 g ZnO	20 ppm	180 min	92.5	[41]
UV-Visible	0.25g ZnO (SA2)	100 ppm (pH 9)	460 min	85	Present work
Sun Light	0.25g ZnO (SA2)	100 ppm (pH 9)	360 min	95	Present work

The ZnO sample SA3 prepared from ethanol solvent has been extra defects greatly de-generates the nano particle size and shape ***[42]*** . The surface morphology and surface defects which are well suitable for Photocatalytic dye degradation. The Table 3 shows the SA2 and SA3 the ZnO nanoparticles are proving to be efficient materials for degrading MB from previous work.

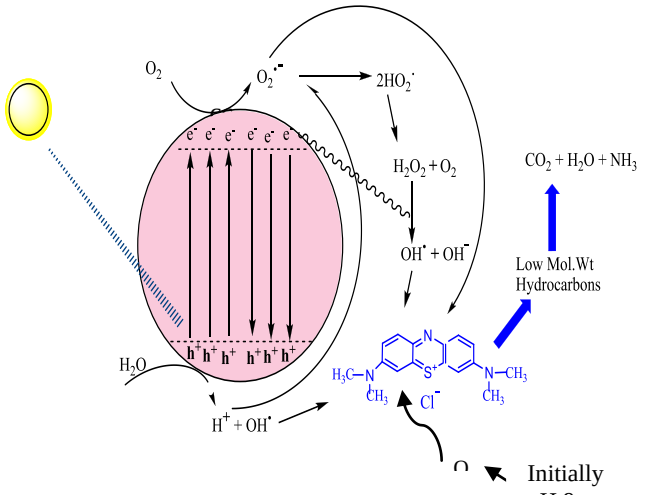

Figure 13. Schematic demonstration on mechanism of photocatalytic dye degradation.

V. AAntimicrobial activity of ZnO

As it is shown a clear inhibition zone, using regular antibiotic disc (30 µg/ml) tetracycline is used as a control and these results shown in Figure 14 and Table 4. The ZnO nanoparticles produce reactive oxygen species which is reacted with a bacterial membrane at room temperature. Divya et al. stated that this bacteria cell membrane is damaged by ZnO nanoparticles that extruded to the part of cytoplasmic substance and causing the kill the bacterium [43]. Dimapilis et al. reported the antimicrobial activity increase in ZnO nanoparticles depends mainly on particle size [44].

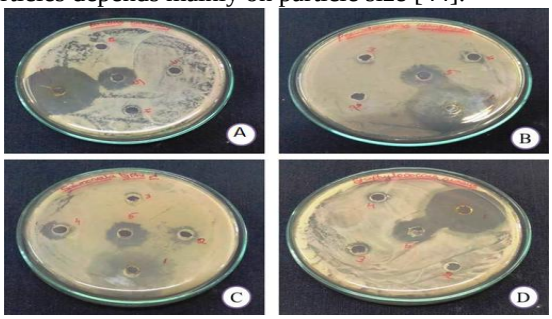

Figure 14. Antibacterial activity of ZnO NPs against (A) p. aeruginosa, (B) b. subtilis, (C) s. typhi and (D) s. aureus

Table 4. Antibacterial activities of the compounds treated against bacterial pathogens

Test organisms	Zone of inhibition in millimeter (in diameter)			
	Positive control			Negative control
	SA2 Sample (µg)		Standard Tetracycline 30µg	
	10	30		
B.substillas(G.P)	-	20	24	-
P. aeruginosa(G.N)	-	29	22	-
S.typhi(G.N)	3	22	21	-
S. aureus(G.P)	-	23	27	-

VI. CONCLUSIONS

In brief, nano-ZnO is prepared by co-precipitation technique using different solvents with and without cetrimide as a surfactant. From the obtained results, solvents and cetrimide has a strong influence on the morphology and also found the notable changes in optical properties of nano-ZnO. The SEM images prove the excellent changes in all sample morphology depends the various solvents and cetrimide. The XRD and PL data indicate the particle size decreases with increase of Surface defects. DRS spectra good agree with band-gap value changes from 3.31 eV to 3.35 eV when the addition of surfactant cetrimide. EDX spectra shows the surface oxygen vacancy in the SA2 and SA3 samples and scavengers studies h+ holes are the main responsible for photocatalytic activities. It has well to correlate the photocatalytic activity mechanism of nano -ZnO demonstrated the excellent degradation of MB under the UV lamp and solar irradiations. The SA2 and SA3 ZnO nano particles are proving to be efficient materials for degrading Methylene blue among the four samples in sunlight 95%. This may be due to the fact that sampled SA2 and SA3 are sized, defects, strain and morphology respectively. The SA3 sample degraded to MB even without the addition of surfactant. Therefore, ethanol acted both as a solvent and stabilizer. The samples SA1 and SA4 show the slow rates of degrading MB due to agglomeration which led to big particle size and good crystallinity of nano-ZnO. In addition, the radical scavenging investigation on the degradation MB when the ZnO created valence band holes are the principle responsive species demonstrating that the MB dyes have an affect the degradation mechanism. The antimicrobial activities of smaller size SA2 nanoparticle sample had a significant performance against both gram-negative bacterias (Pseudomonas aeruginosa and Salmonella typhi) and gram-positive bacterias (Staphylococcus aureus, and Bacillus subtilis) showing the best results. It is noted that nano-ZnO have better respondent against p. aeruginosa compare to other bacterias tested in the present study. Hence, the SA2 sample can be suggested to be an effective medicine to cure or to inhibit the pain, itch and skin disease especially by the bacterial infections.

ACKNOWLEDGMENT

The authors confirm that there are no other conflicts of interest associated with this publication and there has been no significant financial support for this work that could have influenced its outcome. We would like to thank the concern authorities of Sethu Institute of Technology and Engineer S. Jaffer ali for the relentless encouragements.

REFERENCES

1. S. Sun, X. Zhang, Q. Yang, S. Liang, X. Zhang, Z. Yang, Cuprous oxide (Cu2O) crystals with tailored architectures: A comprehensive review on synthesis, fundamental properties, functional modifications and applications, Progress Mater Sci., 2018, 96, 111-173.
2. H. Tong, S.X. Ouyang, Y.P. Bi, N. Umezawa, M. Oshikiri, J.H. Ye, Nano Photocatalytic Materials: Possibilities and Challenges, Adv Mater., 2012, 24, 229-251.

3. D. Beydoun, R. Amal, G. Low, Role of nanoparticles in photocatalysis, J Nanopa Rese., 1999, 1, 439–458.
4. Y. Liao, W. Que, Z. Tang, W. Wang, W. Zhao, Effects of heat treatment scheme on the photocatalytic activity of TiO2 nanotube powders derived by a facile electrochemical process, J Alloys and Comp., 2011, 509, 1054–1059.
5. N.R. Khalid, E. Ahmed, Z. Hong, M. Ahmad, Synthesis and photocatalytic properties of visible light responsive La/TiO 2-graphene composites, Appl Surf Sci., 2012, 263, 254–259.
6. J. Wang, D.N. Tafen, P.J. Lewis, Z. Hong, A. Manivannan, M. Zhi, M. Li, N. Wu, Origin of Photocatalytic Activity of Nitrogen-Doped TiO2 Nanobelts, J American Chem Society., 2009, 131, 12290–12297.
7. L. Amy, Linsebigler, G. Lu, T. John, Yates, Photocatalysis on TiO2 Surfaces: Principles, Mechanisms, and Selected Result, Chemical Reviews., 1995, 95 (3), 735–758.
8. B. Li, Y. Wang, Facile Synthesis and Enhanced Photocatalytic Performance of Flower-like ZnO Hierarchical Microstructures, J Phy Chem C., 2010, 114, 890–896.
9. Karthick, R and Sundararajan, M: "A Reconfigurable Method for Time Correlated MIMO Channels with a Decision Feedback Receiver," International Journal of Applied Engineering Research 12 (2017) 5234
10. . Karthick, R and Sundararajan, M: "PSO based out-of-order (ooo) execution scheme for HT-MPSOC"Journal of Advanced Research in Dynamical and Control Systems 9 (2017) 1969.
11. J. Chen, X. Wen, X. Shi, R. Pan, Synthesis of Zinc oxide/ Activated Carbon Nano-Composites and Photodegradation ofg Rhodamine B, Envi Eng Sci., 2012, 29 (6), 392-398.
12. S. Gayathri, P. Jayabal, M. Kottaisamy, V. Ramakrishnan, Synthesis of ZnO decorated graphene nanocomposite for enhanced photocatalytic properties, J Appl Phy., 2014, 115, 173504-173509.
13. A. Kalita, M.P.C. Kalita, Microstructural, optical, magnetic and photocatalytic properties of Mn doped ZnO nanocrystals of different sizes, Physica B: Phy Cond Matter., 2019, 552, 30-46.
14. Karthick, R and Sundararajan, M: "A novel 3-D-IC test architecture-a review," International Journal of Engineering and Technology (UAE) 7 (2018) 582.
15. M. Pisarcik, M. Lukac, J. Jampilek, F. Bilka, A. Bilkova, L. Paskova, Ferdin, Devinsky, R. Horakova, T. Opravi, Silver nanoparticles stabilised with cationic single-chain surfactants. Structure-physical properties-biological activity relationship study, J Mole Liq., 2018, 272, 60-72.
16. H.J. Zhaia, W.H. Wub, F. Lub, H.S. Wangb, C. Wangb, Effects of ammonia and cetyltrimethylammonium bromide (CTAB) on morphologies of ZnO nano- and micromaterials under solvothermal process, Mat Chem and Phy., 2008, 112, 1024–1028.
17. N. Singh, P. Pandey, F.Z Haque, Effect of heat and time-period on the growth of ZnO nanorods by sol–gel technique, Int J for Light and Electron Optics., 2012, 123 (15), 1340-1342.
18. A. Hamrounia, H. Lachheba, A. Houas, Synthesis, characterization and photocatalytic activity of ZnO-SnO2 nanocomposites, Mat Sci and Eng B., 2013, 178, 1371– 1379.
19. P.V. Gaikwad, R.J. Kamble, S.J.M. Gavade, S.R. Sabale, P.D. Kamble, Magneto-structural properties and photocatalytic performance of sol-gel synthesized cobalt substituted Nisbnd Cu ferrites for degradation of methylene blue under sunlight, Physica B: Phy Cond Matter., 2019, 554, 79-85.
20. K. Ravichandran, P. Philominathan, Comparative Study On Structural And Optical Properties Of Cds Films Fabricated By Three Different Low-Cost Techniques, App Surf Sci., 2009, 255 (11), 5736-5741.
21. Karthick, R and Sundararajan, M: "Design and Implementation of Low Power Testing Using Advanced Razor Based Processor," International Journal of Applied Engineering Research 12 (2017) 6384
22. S. Benramache, B. Benhaoua, N. Khechai, F. Chabane, Elaboration and charac-terization of ZnO thin films, Matériaux Techiques., 2012, 100, 573–580.
23. K.H.S. Kung, K.F. Hayes, Fourier transform infrared spectroscopic study of the adsorption of cetyltrimethylammonium bromide and cetylpyridinium chloride on silica, Langmuir., 1993, 9 (1), 263–267.
24. L.J Bellamy, In The Infrared Spectra of Complex Molecules., New York : Wiley: London Chapman and Hall, 1975.
25. K. Kaviyarasu, P.A. Devarajan, A convenient route to synthesize hexagonal pillar shaped ZnO nanoneedles via CTAB surfactant, Adv. Mat. Letters., 2013, 4 (7), 582-585.
26. J.C. Sin, S.M. Lam, K.T. Lee, A.B. Mohamed, Preparation and photocatalytic properties of visible light-driven samarium-doped ZnO nanorods, Ceramics Inter., 2013, 39, 5833–5843.
27. Y. Ku, Y.H. Huang, Y.C. Chou, Preparation and characterization of ZnO/TiO2 for the photocatalytic reduction of Cr(VI) in aqueous solution, J Mol Catal A: Chem., 2011, 18-22, 342–343.
28. I. Weissbuch, V.Y. Torbeev, L. Leiserowitz, M. Lahav, Solvent effect on crystal polymorphism: why addition of methanol or ethanol to aqueous solutions induces the precipitation of the least stable beta form of glycine, Angewandte Chemical International., 2005, 44, 3226-3229.
29. T. Thilagavathi, D. Geeth, Nano ZnO structures synthesized in presence of anionic and cationic surfactant under hydrothermal process, Appl Nano sci., 2014, 4, 127–132.
30. H.R. Pouretedal, A. Kadkhodaie, Synthetic Ceo2 Nanoparticle Catalysis Of Methylene Blue Photodegradation: Kinetics And Mechanism, Chinese J Catalysis., 2010, 31 (11), 1328-1334.
31. H.H. Li, S. Yin, Y.H. Wang, T. Sato, Efficient persistent photocatalytic decomposition of nitrogen monoxide over a fluorescence-assisted CaAl2O4:(Eu, Nd)/(Ta, N)-codoped TiO2/Fe2O3, Appl Catal B Environ., 2013, 132-133, 487–492.
32. Y. Wang, K. Deng, L. Zhang, Visible Light Photocatalysis of BiOI and Its Photocatalytic Activity Enhancement by in Situ Ionic Liquid Modification, J Phys Chem C., 2011, 115, 14300–14308.
33. M.S. Gohari, A.H. Yangjeh, Novel magnetically separable Fe3O4@ZnO/AgCl nanocomposites with highly enhanced photocatalytic activities under visible-light irradiation, Sepa Purif Technol., 2015, 147, 194–202.
34. J. Wang, W.J. Jiang, D. Liu, Z. Wei, Y.F. Zhu, Photocatalytic performance enhanced via surface bismuth vacancy of Bi6S2O15 core/shell nanowires, Appl Catal B Environ., 2015, 176, 306–314.
35. A. Houas, H. Lachheb, M. Ksibi, E. Elaloui, C. Guillard, J.M. Herrmann, Photocatalytic degradation pathway of methylene blue in water, App Catalysis B: Envir., 2001, 31, 145–157.
36. Li, J.; Lu, G.; Wang, Y.; Guo, Y.; Guo, Y, A high activity photocatalyst of hierarchical 3D flowerlike ZnO microspheres:Synthesis, characterization and catalytic activity, J Colloid and Inter Sci., 2012, 377, 191–196.
37. B.G. Ankamwar, V.B Kamble, J.I. Annsi, L.S. Sarma, C.M. Mahajan, solar Photocatalytic Degradation of Methylene Blue by ZnO Nanoparticles, J Nanosci Nanotech., 2017, 17, 1185-1192.
38. N. Chekir, O. Benhabilesa, D. Tassalitab, N.A. Laoufib, F. Bentahar, Photocatalytic degradation of methylene blue in aqueous suspensions using TiO2 and ZnO, Desali Water Treat., 2015, 57 (13), 6141-6147.
39. H.R. Mardani, M. Forouzani, M. Ziari, P. Biparva, Visible light photo-degradation of methylene blue over Fe or Cu promoted ZnO nanoparticles, Spectrochimica Acta Part A: Molec and Biomole Spec., 2015, 141, 27–33.
40. A.M. Oda, A. Salih, S. Hadi, A. Jawad, A. Sadoon, Y. Fahim, A. Fadhil, Photocatalytic decolorization of methylene blue dye by zinc oxide powder, J Babylon University/Pure and Appl Sci., 2014, 9 (22), 2508-2515.
41. A. Balcha, O.P. Yadav, T. Dey, Photocatalytic degradation of methylene blue dye by zinc oxide nanoparticles obtained from precipitation and sol-gel methods, Env Sci Pollut Res., 2016, 23 (24), 25485-25493.
42. M.A. kumar, S. Muthukumaran, Effect of solvents on the structural, optical and morphological properties of Zn0.96Cu0.04O nanoparticles, J Mater Sci: Mater Electron., 2013, 24, 4050–4059.
43. M.J. Divya, C. Sowmia, K. Joona, K.P. Dhanya, Synthesis of zinc oxide nanoparticle from Hibiscus rosa-sinensis leaf extract and investigation of its antimicrobial activity, Res J Pharm Biol Chem., 2013, 4 (2), 1137-1142.
44. A.S. Dimapilis, C.S. Hsu, R.M.O. Mendoza, M.C. Lu, Zinc oxide nanoparticles for water disinfection, Sustain Envir Rese., 2018, 28 (2), 47-56.

AUTHORS FROFILE

Mr. S. Sheik Mydeen, is currently working as Assistant Professor in the Department of Chemistry, Sethu institute of technology, Virudhunagar – 626 115, India. His field of research includes Nanomaterials, environmental and photocatalytic applications. He has 14 years teaching experience. Dr. M. Kottaisamy has done his Doctoral Degree at Bharathidasan University, published more than 80 research articles in international journals, 5 book chapters and presented 60 papers in national and international conferences. He has 29 years teaching and research experience.

Dr.V.S.Vasantha, has interests in various fields of Biosensors, Natural Products Isolation, Fuel Cell, Electroplating, Corrosion, Natural Products Chemistry, and Electrochemistry. She has published more than 60 research articles in international journals, 1 book chapter and presented 25 papers in national and international conferences. She has 30 years teaching and research experience.